

ACCEPTED MANUSCRIPT • OPEN ACCESS

Risk and reward of the global truffle sector under predicted climate change

To cite this article before publication: Tomas Cejka *et al* 2022 *Environ. Res. Lett.* in press <https://doi.org/10.1088/1748-9326/ac47c4>

Manuscript version: Accepted Manuscript

Accepted Manuscript is “the version of the article accepted for publication including all changes made as a result of the peer review process, and which may also include the addition to the article by IOP Publishing of a header, an article ID, a cover sheet and/or an ‘Accepted Manuscript’ watermark, but excluding any other editing, typesetting or other changes made by IOP Publishing and/or its licensors”

This Accepted Manuscript is © 2022 The Author(s). Published by IOP Publishing Ltd.

As the Version of Record of this article is going to be / has been published on a gold open access basis under a CC BY 3.0 licence, this Accepted Manuscript is available for reuse under a CC BY 3.0 licence immediately.

Everyone is permitted to use all or part of the original content in this article, provided that they adhere to all the terms of the licence <https://creativecommons.org/licenses/by/3.0>

Although reasonable endeavours have been taken to obtain all necessary permissions from third parties to include their copyrighted content within this article, their full citation and copyright line may not be present in this Accepted Manuscript version. Before using any content from this article, please refer to the Version of Record on IOPscience once published for full citation and copyright details, as permissions may be required. All third party content is fully copyright protected and is not published on a gold open access basis under a CC BY licence, unless that is specifically stated in the figure caption in the Version of Record.

View the [article online](#) for updates and enhancements.

1 Risk and reward of the global truffle sector under predicted 2 climate change

3
4 Tomáš Čejka^{1,2*} | Elizabeth Isaac³ | Daniel Oliach^{4,5} | Fernando Martínez-Peña^{6,7} |
5 Simon Egli⁸ | Paul Thomas⁹ | Miroslav Trnka^{1,10} | Ulf Büntgen^{1,2,3,8}
6

7 *¹Department of Climate Change Impacts on Agroecosystems, Global Change Research Institute of the
8 Czech Academy of Sciences, Bělidla 986/4, 603 00 Brno, Czech Republic. ²Department of Geography,
9 Faculty of Science, Masaryk University, Kotlářská 2, 602 00 Brno, Czech Republic. ³Department of
10 Geography, University of Cambridge, Downing Place CB2 3EN, Cambridge, United Kingdom. ⁴Forest
11 Science and Technology Centre of Catalonia (CTFC), Crta. Sant Llorenç de Morunys km 2, E-25280
12 Solsona, Spain. ⁵Department of Crop and Forest Science, University of Lleida, Alcalde Rovira Roure
13 191, 25198 Lleida, Spain. ⁶Agrifood Research and Technology Centre of Aragon CITA, Avda Montañana
14 930, E-50059 Zaragoza, Spain. ⁷European Mycological Institute EGTC-EMI, E-42003 Soria, Spain.
15 ⁸Swiss Federal Institute for Forest, Snow and Landscape Research WSL, Zürcherstrasse 111, 8903
16 Birmensdorf, Switzerland. ⁹Faculty of Natural Sciences, University of Stirling, FK9 4LA, Stirling, United
17 Kingdom. ¹⁰Department of Agrosystems and Bioclimatology, Faculty of AgriSciences, Mendel
18 University, Zemědělská 1, 613 00 Brno, Czech Republic.*

19
20 *corresponding author: tomas.cejka.94@gmail.com, +420 720 490 258, ORCID 0000-0002-9254-8000

21
22 Co-author's contact addresses: EI (eli23@cam.ac.uk), DO (daniel.oliach@ctfc.es), FMP
23 (fmartinezpe@cita-aragon.es), SE (simon.egli@hispeed.ch), PT (paul@plantationsystems.com), MT
24 (mirek_trnka@yahoo.com), UB (ulf.buentgen@geog.cam.ac.uk)
25

26 **Keywords:** adaptation strategies, agricultural drought, climate models, irrigation systems, price
27 estimates, production risk, truffle industry

28 **Abstract**

29 Climate change has been described as the main threat for the cultivation and growth of truffles,
30 but hydroclimate variability and model uncertainty challenge regional projections and
31 adaptation strategies of the emerging sector. Here, we conduct a literature review to define the
32 main Périgord truffle growing regions around the world and use 20 global climate models to
33 assess the impact of future trends and extremes in temperature, precipitation and soil moisture
34 on truffle production rates and price levels in all cultivation regions in the Americas, Europe,
35 South Africa, and Australasia. Climate model simulations project 2.3 million km² of suitable
36 land for truffle growth will experience 50% faster aridification than the rests of the global land
37 surface, with significantly more heat waves between 2070 and 2099 CE. Overall, truffle
38 production rates will decrease by ~15%, while associated price levels will increase by ~36%.
39 At the same time, a predicted increase in summer precipitation and less intense warming over
40 Australasia will likely alleviate water scarcity and support higher yields of more affordable
41 truffles. Our findings are relevant for truffle farmers and businesses to adapt their irrigation
42 systems and management strategies to future climate change.

44 **1 Introduction**

45 Increasing temperature means and changes in precipitation totals are likely to affect the
46 productivity and functioning of ecosystems and agriculture in the 21st century (Gornall et al.,
47 2010; Challinor et al., 2014; Ray et al., 2015). Regions with a Mediterranean climate, such as
48 southern Europe, the western United States, central Chile, South Africa, and parts of Australasia
49 are particularly vulnerable to anthropogenic warming (Mann and Gleick, 2015; Cramer et al.,
50 2018; Rojas et al., 2019). The projected drying in many of those regions poses an unprecedented
51 economic threat to specialized high-value crops (Rojas et al., 2019; Zhang and Delworth, 2018),
52 such as grapes (Cook and Wolkovich, 2016; Morales-Castilla et al., 2020), olives (Ponti et al.,

1
2
3 53 2015) and truffles (Büntgen et al., 2012; Le Tacon et al., 2014; Thomas and Büntgen, 2019).
4
5 54 The cultivation of Périgord (*Tuber melanosporum* Vittad.) truffles and, to a lesser extent also
6
7 55 the Burgundy (*Tuber aestivum*) truffles, benefits the primary, tertiary and quaternary economic
8
9 56 sectors at different geographical scales. To date, the emerging truffle ‘industry’ generates
10
11 57 hundreds of millions of Euros annually (Oliach et al., 2020a), increases land and property value,
12
13 58 promotes myco-tourism (Büntgen et al., 2017), and stimulates interdisciplinary research
14
15 59 (Büntgen and Egli, 2014). An ever-growing number of plantations of this most sought-after
16
17 60 ectomycorrhizal ascomycete, i.e., the black truffle, can strengthen local economies and may
18
19 61 even enhance ecological stability, not only in the traditional trufficulture areas of southern
20
21 62 Europe (Büntgen et al., 2017), but also in Mediterranean parts of the Americas, South Africa
22
23 63 and Australasia (Hall et al., 2003; Reyna and Garcia-Barreda, 2014). Under current and
24
25 64 projected climate change, the truffle sector, however, requires advanced irrigation systems to
26
27 65 reduce the risk of drought-induced fluctuations in the quantity and quality of their annual
28
29 66 harvests (Büntgen et al., 2012; Thomas and Büntgen, 2019). Understanding the direct and
30
31 67 indirect effects of a warmer and drier climate on the intertwined global truffle sector is
32
33 68 fundamental to refine adaptation strategies and inform decision-making at a wide range of
34
35 69 relevant ecological, socio-political and economic scales.
36
37
38
39
40
41

42 70 Here, we present a literature review of biogeographical, ecophysiological and climatological
43
44 71 information about the Périgord black truffle. We conduct a meta-analysis of all previously
45
46 72 published truffle data to define the main truffle growing regions around the world (hereinafter
47
48 73 truffle growing regions; TGRs). We apply different scenarios from 20 state-of-the-art global
49
50 74 climate models (GCMs) to quantify trends and extremes in seasonal temperature means,
51
52 75 precipitation totals and soil moisture levels of the TGR until 2100 CE and compare those data
53
54 76 against projections for the rest of the global land surface. To estimate the impacts of projected
55
56 77 climate change on truffle production, we calculate the area affected by climate outside the
57
58
59
60

1
2
3 78 acceptable ecological limit of truffle growth and combine model projections with historical
4
5 79 truffle market observations to estimate future changes in truffle production rates and price
6
7
8 80 levels.
9

10 81

11 82 **2 Data and Methods**

12 83 **2.1 Truffle growing regions**

13
14
15
16
17 84 To date, no global database of TGRs has been compiled, primarily because of the secrecy of
18
19 85 the location of truffle plantations, which reflects the reluctance of sharing specific information
20
21 86 by truffle farmers and hunters. In order to define the global distribution of the main Périgord
22
23 87 TGRs that substantially contribute to international markets, we reviewed peer-reviewed
24
25 88 scientific articles, monographs, technical notes, conference abstracts and posters (Tab. S1). All
26
27 89 information was published after 2010, either in indexed databases or on the truffle growers'
28
29 90 association websites. Of the dozens of relevant publications that included the search words
30
31 91 'truffle' or 'truffle plantation' or 'truffle cultivation' in conjunction with toponyms, only ten
32
33 92 articles contained useful information about specific TGRs. While we restricted our focus to
34
35 93 those regions in which production has been reported (Tab. S1), we excluded all regions with
36
37 94 established plantations lacking any recent harvest (e.g., China; C. Colinas, pers. comm.) or
38
39 95 showing globally insignificant production rates (e.g., Morocco, Israel, the United Kingdom,
40
41 96 eastern United States). Finally, we neglected occasional individual truffle findings and
42
43 97 theoretically suitable areas for truffle growth (Thomas and Büntgen, 2017), such as the region
44
45 98 between Texas and Virginia (Lefevre et al., 2012).

46
47
48
49 99 To delineate and digitise all TGRs, we used the QGIS ver. 3.16 (QGIS, 2021) to produce a
50
51 100 shapefile in which polygon features represent the TGRs. In Europe (Spain, Italy and France),
52
53 101 Chile, South Africa and New Zealand, we defined boundaries based on 1st-level administrative
54
55 102 subdivisions (AS). In the United States where this administrative scale corresponds with
56
57
58
59
60

1
2
3 103 individual states, we used 2nd-level AS instead. Shapefile data on both spatial levels are
4
5 104 available at the 'Database of Global Administrative Areas' (see SI). While the 1st-level AS in
6
7 105 Australia corresponds to large territories and the 2nd-level AS (small local government bodies)
8
9 106 is too small for resolution of GCMs, we defined TGRs by temperate and Mediterranean climate
10
11 107 zone according to Köppen. These groups sufficiently cover the spatial distribution of currently
12
13 108 operating truffle plantations (Tab. S1) and are considered suitable for truffle cultivation
14
15 109 (Malajczuk and Amaranthus, 2007). Data on climate zones are freely available at Australian
16
17 110 Bureau of Meteorology (see SI). To clarify the relationship between temperate (all subtypes:
18
19 111 Cs, Cw, Cf) and Mediterranean climate (only Cs), we provided the corresponding subtypes to
20
21 112 each TGR (Beck et al., 2018) (Tab. S2). Data for the climate diagrams based on instrumental
22
23 113 records ('present climate') are available at NOAA (see SI).
24
25
26
27
28
29
30

31 115 **2.2 Data on truffle ecology and production, and climate variability**

32
33 116 Périgord truffles grow at sites with an average annual temperature of around 12 °C and
34
35 117 precipitation totals of approximately 780 mm. The optima for the warmest and coldest months
36
37 118 (July and January) are 20.5 °C and 3.8 °C, respectively. Summer precipitation totals must not
38
39 119 fall below 140 mm (Čejka et al., 2020). Although Périgord truffles are harvested in winter from
40
41 120 around November to March, fruitbody formation likely starts as early as the previous spring,
42
43 121 after mycorrhizal colonisation of the host tree roots and mycelium formation (Garcia-Barreda
44
45 122 et al., 2020). Between spring and late summer, the growth and maturation (peridium and gleba
46
47 123 development) continue. This process mainly depends on the amount of water in the soil and
48
49 124 host plants, although excess precipitation in the cooler autumn season may affect truffle
50
51 125 harvests negatively (Büntgen et al., 2019). By the same token, the increased frequency of
52
53 126 climatic extremes, such as drought spells and sub-zero temperatures, often impair future
54
55 127 harvests. In addition to reduced truffle yields, prolonged summer drought can affect fruitbody
56
57
58
59
60

1
2
3 128 maturation, while winter frosts may cause peridium rupture, especially if the truffle contains
4
5 129 large amounts of water (Thomas and Büntgen, 2019).
6

7
8 130 Since growth and ripening of Périgord truffles, which are mostly found in the topsoil layer,
9
10 131 depend on natural summer rainfall and temperature (Büntgen et al., 2019), we selected three
11
12 132 modelled climate variables for the summer season: temperature (Kelvin), precipitation flux
13
14 133 ($\text{kg}\cdot\text{m}^{-2}\cdot\text{s}^{-1}$), and moisture in the upper ~ 10 cm of the soil column ($\text{kg}\cdot\text{m}^{-2}$). This last variable
15
16 134 was preferred over column-wide moisture because GCMs vary in soil depth. That, in addition
17
18 135 to the non-uniform vertical distribution of soil water, makes GCMs not comparable (Berg et
19
20 136 al., 2016). While climate estimates of temperature and precipitation were derived from a set of
21
22 137 20 GCMs, soil moisture was limited by the availability of only 17 models (Tab. S3). All GCMs
23
24 138 used in this study contributed to CMIP5 as part of the IPCC Assessment Report 5 (Flato and
25
26 139 Marotzke, 2013), and are available from the World Data Center for Climate (see SI). Our
27
28 140 preference for GCMs over regional climate models is described in the online SI. To estimate a
29
30 141 wide range of climate change impacts on TGRs throughout the 21st century (2006–2100 CE),
31
32 142 we used both a ‘moderate’ and ‘severe’ climate scenario represented by the RCP_{4.5} and RCP_{8.5},
33
34 143 respectively. In ensuring consistency and avoiding over-representing the forced responses of
35
36 144 GCMs that submitted more realisations to the CMIP5 dataset, we employed only the first
37
38 145 ensemble member from each model (r1i1p1). To process the GCMs, as well as any other climate
39
40 146 data (NetCDF format), we used the Climate Data Operator (CDO) 1.9.8 software (Schulzweida,
41
42 147 2019). For a detailed description of the processing and bias correction of the data using CDO,
43
44 148 see the online SI.
45
46
47
48
49

50
51 149 Using the QGIS ver. 3.10 (QGIS, 2021) we exported vertices’ coordinates of all shapefile’s
52
53 150 polygons into a delimited text file, which was then imported into the CDO to extract future
54
55 151 projections of climate variables in TGRs. To remove oceanic regions from all variables, we
56
57 152 applied a similar procedure to the global landmass shapefile (see SI) and created a mask over
58
59
60

1
2
3 153 which we computed the area average, which we hereafter considered to be the global mean.
4
5 154 Since the CRU and GLDAS-2.1 baseline datasets do not spatially cover high-latitudes in the
6
7 155 Southern Hemisphere, preventing local bias-correction, Antarctica was excluded from the
8
9
10 156 global landmass. When calculating a mean of each timestep (summer season) for TGRs and the
11
12 157 globe, we accounted for grid-specific weights derived from the cell area of the Gaussian grid.
13
14 158 Finally, with summer data being related to June–August (JJA) and December–February (DJF)
15
16
17 159 in the Northern and Southern Hemispheres, respectively, we computed estimates of seasonal
18
19 160 means from monthly temperature and soil moisture data, and seasonal sums from daily
20
21 161 precipitation totals. Since the austral summer data for 2100 terminate by the end of the year, we
22
23 162 excluded 2100 from our analysis.

24
25
26 163 We examined the direct response of the truffle sector in each TGR to projected climate
27
28 164 change using the impact analysis. We estimated Périgord truffle price levels for each TGR for
29
30 165 the late 21st century based on historical data from the world's two most important truffle
31
32 166 exporting countries in Europe (see Data analysis). We used historical prices from wholesale
33
34 167 markets in France (1995–2020/21) provided by Agrimer, France (<https://rnm.franceagrimer.fr>),
35
36 168 and Spain (1997/98–2020/21) compiled in 2021 from multiple sources including Reyna (2012),
37
38 169 Oliach et al. (2020b) and Teruel Truffle Growers Association
39
40 170 (<https://trufadeteruel.com/atrufer/>). Similarly, we estimated Périgord truffle production rates in
41
42 171 each TGR for the late 21st century based on historical records from Spain, France, and Italy
43
44 172 (Groupement Européen Truffe et Trufficulture GETT; Spanish Federation of Truffle Growers
45
46 173 Associations FETT; French Federation of Truffle Growers; Oliach et al., 2021). Therefore, we
47
48 174 were also able to provide estimates of future price levels and production rates for each TGR
49
50 175 (see Data Analysis and Results). However, we did not include historical records from non-
51
52 176 traditional TGRs, because local truffle cultivation has only recently begun in some regions.
53
54 177 That, in addition to exponential truffle growth reflecting the number of plantations rather than
55
56
57
58
59
60

1
2
3 178 natural variability in precipitation, makes reliable predictions difficult. Estimating future
4
5 179 parameters in non-traditional TGRs is further problematic due to the lack of official and
6
7 180 homogenised records. To the best of our knowledge, the only existing truffle harvest data are
8
9 181 limited to personal inventories and biased towards a small number of plantations.
10
11
12 182

13 14 183 **2.3 Statistical analysis and modelling**

15
16
17 184 To detect long-term trends in the climate projections, we applied a non-seasonal Mann-Kendall
18
19 185 test on the bias-corrected 2006–2099 anomalies relative to the 2006–2020 baseline mean
20
21 186 (Mann, 1945). This non-parametric statistical test is commonly used to detect increasing or
22
23 187 decreasing trends over time for many types of data, including groundwater, water quality,
24
25 188 streamflow, lake levels, temperature, and precipitation. In terms of functionality, the Mann-
26
27 189 Kendall statistics were determined by the ranks of the original values and do not require
28
29 190 homoskedasticity and normal distribution (Wang et al., 2020).
30
31
32

33 191 Moreover, we observed if climate parameters are likely to get significantly more or less
34
35 192 variable until the end of 21st century by testing heteroscedasticity of the bias-corrected area-
36
37 193 average of TGRs and the remaining global land surface between 2020 and 2039 and the distant
38
39 194 future from 2070–2099 CE. We used prior-ANOVA non-parametric Levene's test (Levene,
40
41 195 1960; Tab. S4), after inspecting (non-)normality via the Shapiro-Wilk test (Shapiro and Wilk,
42
43 196 1965) (Tab. S5). We used the Shapiro-Wilk test because it is not as affected by ties as
44
45 197 the Anderson-Darling test, and we chose Levene's test over Bartlett test because it is less
46
47 198 sensitive to departures from the mean. To understand spatial climatic extremes, we developed
48
49 199 plots showing the distribution of standard deviation differences of annual variability between
50
51 200 the early (2010–2039) and late (2070–2099) period for each grid cell in each TGR.
52
53
54

55
56 201 Based on a strong dependency of winter Périgord truffle production on previous summer
57
58 202 precipitation ($p < 0.00001$; Büntgen et al., 2019), and the adverse effect of heatwaves on truffle
59
60

1
2
3 203 growth (Garcia-Barreda et al., 2020), we developed multiple linear regression (MLR) models
4
5 204 with two independent variables. These were represented by summer precipitation and the heat
6
7 205 index of the warmest months (July and January). The latter is a physiological parameter
8
9 206 combining the effect of air temperature and relative humidity. However, since the heat index is
10
11 207 not usually measured, we used the July/January temperature and relative humidity to calculate
12
13 208 this parameter according to the conventional equation (see SI). Historical and projected relative
14
15 209 humidity data were obtained from ERA5 (reanalysis) and World Data Center for Climate
16
17 210 (GCMs), respectively (see Data availability). Using a common period of 24 years from
18
19 211 1997/98–2020/21, we calculated five MLR models (Tabs. S6–10) between historical climate
20
21 212 (CRU TS4.05 or ERA5) and national price levels (Spain and France) and production rates
22
23 213 (including Italy). We applied three models for production rates and two models for price levels
24
25 214 on bias-corrected future climate data to estimate these parameters in each TGR for a three
26
27 215 successive 24-year periods: 1997–2020, 2021–2044 and 2076–2099. Both independent
28
29 216 variables were used in all five MLR models except for the association between Spanish
30
31 217 production and the heat index, which lacked correlation ($r = -0.01$) and showed
32
33 218 multicollinearity. We then used the sum of the three and the average of the two sets of modelled
34
35 219 production and price values, respectively. We did not standardize any of the data used.
36
37
38
39
40
41
42
43

221 3 Results

222 Seven TGRs on both hemispheres cover ~2.3 million km² of arable land (Fig. 1, Tab. S11).
223 With ~970,000 km², almost half of the suitable land for global truffle cultivation is located in
224 southern Europe between ~35.8 and 47.7 °N. Based on the 1981–2010 climatology, the mean
225 summer temperature and total precipitation in this area (20.4 °C and 137 mm) are similar to
226 Australia (20.3 °C and 162 mm) and South Africa (21.2 °C and 186 mm), which represent the
227 second and third largest TGRs (~800,000 and 230,000 km²) (Fig. 1). With an average summer

1
2
3 228 temperature between ~14 and 18 °C, and a wide range of precipitation totals from ~60–250
4
5 229 mm, the remaining 14% of TGRs are distributed across Chile (~150,000 km²), New Zealand
6
7 230 (~110,000 km²), and the western United States (~60,000 km²) (Fig. 1, Tab. S11).

9
10 231 All TGRs are almost certain to undergo changes in summer temperature means, precipitation
11
12 232 totals and the availability of moisture in the topsoil during the 21st century (Fig. 2). Averaging
13
14 233 over all TGRs trajectories, summer temperatures under RCP_{8.5} will increase at a rate
15
16 234 comparable to the global land average (~0.6 °C per decade). However, significant differences
17
18 235 exist between regions. Europe is the fastest warming region, where decadal temperature means
19
20 236 rise at ~0.7 °C (RCP_{8.5}) (Fig. 2). Other regions are warming comparably or more slowly than
21
22 237 the rest of the global land surface (~0.4 °C per decade under RCP_{8.5}), excluding Antarctica. In
23
24 238 contrast to the global precipitation increase (+4 % by the end of 21st century), most TGRs are
25
26 239 projected to experience long-term drying under the high-emission scenario, especially Europe
27
28 240 (-31 %), the United States (-25 %) and Chile (-62 %). Only eastern South Africa (both RCPs)
29
30 241 and Australasia (RCP_{8.5}) are likely to mitigate water shortage due to future precipitation
31
32 242 increases (+8 and 9 % under RCP_{8.5}) (Fig. 2). Projections for Australasia are also not exhibiting
33
34 243 any significant trends (RCP_{8.5}) for the moisture content in the upper soil layer. The upper soil
35
36 244 moisture content in all other TGRs, however, is expected to decline ~50 % faster compared to
37
38 245 the rest of the global land surface (RCP_{8.5}).

39
40 246 Projected trends for RCP_{8.5} associated with distribution shifts in climate parameters are
41
42 247 likely to increase the frequency of extreme summer temperatures in all TGRs ($p < 0.05$; Fig. 3).
43
44 248 This trend will be particularly pronounced in north-eastern Australia (Fig. 3g), where year-to-
45
46 249 year variability in precipitation totals between the early and late periods (2020–39 versus 2070–
47
48 250 99) rises substantially (SD +15 mm/m²). A less distinct but still positive SD difference is
49
50 251 apparent in Europe (SD +5 mm/m² in Spain and France), the United States (SD +5 mm/m²),
51
52 252 western Australia (SD +5 mm/m²) and New Zealand (SD +10 mm/m²; Fig. 3c-d-g). The
53
54
55
56
57
58
59
60

1
2
3 253 interannual variability in topsoil moisture is expected to be more stable in all TGRs (Fig. 3b),
4
5 254 but specific regions such as central Spain, eastern South Africa, south-eastern Australia and
6
7 255 New Zealand will be subject to greater variability at the end of this century (SD +0.2–0.4 L/m²
8
9
10 256 on average).

11
12 257 Our MLR models estimate that truffle prices will increase by an average of 10% between
13
14 258 2021 and 2044, with only Chile experiencing a 6% decline (Fig. 4). By the end of the 21st
15
16 259 century (2076–2099), truffles are projected to become on average 36% more expensive, except
17
18 260 for those coming from Chile and New Zealand, where prices could decrease by ~7 and 75 %,
19
20 261 respectively. Although production rates are projected to decline by only ~5 % (TGR average)
21
22 262 from 2021–2044, by the end of the 21st century this parameter will decline by 14%. With
23
24 263 projected production losses of 39%, 56% and 81%, respectively, plantations in Europe, the
25
26 264 United States and Chile are likely to be most affected. On the other hand, estimates in
27
28 265 Australasia will be comparable to current rates (1997–2020). Moreover, given the projected
29
30 266 climate extremes, price levels and production rates by the end of the 21st century are projected
31
32 267 to be more variable and therefore uncertain in many TGRs than in the 2021–2044 period (Fig.
33
34 268 4).

35
36
37
38
39
40 269

41 270 **4 Discussion**

42 271 **4.1 Climate risk**

43
44
45 272 A subtropical high-pressure ridge between spring and autumn forms the Mediterranean climate
46
47 273 of all TGRs, and most of the annual precipitation supply depends on mid-latitude westerly
48
49 274 winds in winter. With a warming-induced strengthening of the mid-latitude jet stream and a
50
51 275 reduction of land–sea temperature gradients that maintain subtropical anticyclonic blocking and
52
53 276 prolong summer droughts (Tuel and Eltahir, 2020), the winters are likely to shorten, and
54
55 277 precipitation totals are expected to decline in many TGRs (Cramer et al., 2018). Exceeding
56
57
58
59
60

1
2
3 278 previous calculations by about ~15–20% (Jacob et al., 2014), JJA precipitation totals in
4
5 279 southern Europe are predicted to decrease by almost ~30%. That, in addition to a predicted
6
7 280 increase of JJA temperatures ~20% faster than the global average (Fig. 2 and Cramer et al.,
8
9 281 2018), will significantly accelerate soil drying by the end of the 21st century. Similar stressors
10
11 282 will exacerbate future drought in the United States' TGRs (Mann and Gleick, 2015), and
12
13 283 increasing temperatures, decreasing precipitation, and soil aridification in central Chile will
14
15 284 likely lead to ~40% drier summer conditions from DJF by the end of the 21st century
16
17 285 (Araya-Osses et al., 2020).

18
19 286 Future summer warming is projected for the whole of South Africa, although hydroclimatic
20
21 287 conditions differ between the west and the east of the country (Roffe et al., 2019). At the western
22
23 288 coast (Western Cape), where the climate is usually drier (Roffe et al., 2019), soil moisture
24
25 289 content and precipitation totals in the austral summer and winter are expected to decrease over
26
27 290 the 21st century (Fig. 2 and Pascale et al., 2020). This, as well as the observed decline in winter
28
29 291 precipitation across eastern South Africa in the past century (Net et al., 2009), is in principle
30
31 292 due to the drying and shifting of subtropical high-pressure ridge towards the pole (Rojas et al.,
32
33 293 2019; Pascale et al., 2020). In contrast, summer precipitation in eastern South Africa (KwaZulu-
34
35 294 Natal) exhibits a positive trend under the influence of the 'warm' Agulhas current bringing
36
37 295 more air moisture (Beal et al., 2011; Fig. 2). This is comparable with downscaled climate
38
39 296 projections indicating increasing summer precipitation in parts of east-central South Africa
40
41 297 (Hewitson and Crane, 2006; Almazroui et al., 2020), probably caused by intensified short-term
42
43 298 heavy precipitation (Dosio et al., 2019).

44
45 299 With future warming, projections for summer precipitation based on our GCMs' ensemble
46
47 300 mean reveal non-significant trends for western Australia over the 21st century (Fig. 2), probably
48
49 301 because of low agreement between the existing GCMs (Raut et al., 2017). Some of these climate
50
51 302 models, however, project a slight increase in summer precipitation in eastern Australia, which
52
53
54
55
56
57
58
59
60

1
2
3 303 is consistent with the ensemble mean used in this study (Fig. 2 and Timbal et al., 2017). In
4
5 304 contrast, comparison between historical (1986–2005 CE) and future (2080–2099 CE) periods
6
7 305 suggests that summer precipitation totals will increase by only 1%. (Timbal et al., 2017).
8
9
10 306 Positive trends in summer precipitation have been suggested to originate from the
11
12 307 intensification of short-term heavy rainfall events at timescales of hours to days (Dey et al.,
13
14 308 2019). Either way, decreasing water content in soil during summer in both Australian TGRs
15
16 309 (RCP_{4.5}; Fig. 2) corresponds with an annual decline in precipitation, particularly in winter (JJA),
17
18 310 when most precipitation occurs (Dey et al., 2019; Delworth and Zeng, 2014). A decrease of
19
20 311 winter precipitation is also projected for New Zealand’s TGRs in the lowland east, as opposed
21
22 312 to those plantations at higher elevations in the west, where precipitation is predicted to increase.
23
24 313 However, summer precipitation is projected to increase in New Zealand, but decrease in the
25
26 314 western part of this country. Fluctuating projected precipitation across New Zealand and a
27
28 315 projected stability of soil moisture content are associated with a decreasing pace of westerly
29
30 316 winds (Ministry for the Environment, 2018), and an increase in the frequency rather than the
31
32 317 intensity of precipitation (Sansom and Renwick, 2007).
33
34
35
36

37 318 Future warming will increase the frequency and intensity of extreme summer temperatures
38
39 319 in most of the TGRs (Fig. 3). Comparison of measured and predicted climate data from Europe
40
41 320 (1961–1990 versus 2071–2100 CE) shows that heatwaves are likely to become twice to five
42
43 321 times as long, and their frequency will increase from one every 3–5 summers to about 2–3
44
45 322 heatwaves per season (Fischer and Schär, 2010). In the United States, the frequency of
46
47 323 heatwaves associated with longer drought episodes will double after 2050 CE, compared to the
48
49 324 earlier period 1950–2000 (Cook et al., 2015). In the Southern Hemisphere, increasing extremes
50
51 325 of summer temperature and soil moisture content associated with intensified El Niño Southern
52
53 326 Oscillation (ENSO) in the 21st century will cause more frequent heatwaves and longer drought
54
55 327 spells in central Chile (Cai et al., 2020), South Africa (Pascale et al., 2020), and western
56
57
58
59
60

1
2
3 328 Australia (Andrys et al., 2017). Even where the influence of ENSO is relatively minor, extreme
4
5 329 summer temperatures in eastern Australia are expected to rise (King et al., 2017), and heatwaves
6
7 330 in late-21st century are predicted to be common for New Zealand, likely due to low wind speeds
8
9 331 associated with unusually positive phases of the South Annual Mode (Salinger et al., 2019).
10
11 332 While a more detailed discussion of possible drivers behind projected climate conditions is
12
13 333 beyond the scope of this study, the uncertainty associated with the GCMs appears crucial for
14
15 334 further research (see our expansion on GCMs uncertainty in SI).
16
17
18
19
20

335

21 336 **4.2 Climate adaptation**

22
23 337 As with other fungal species (Karavani et al., 2018; Diez et al., 2013; Kausrud et al., 2012),
24
25 338 anthropogenic climate change will exert regionally disproportionate effects on the quantity and
26
27 339 quality of truffle yields in the 21st century. With the warm period largely stimulating truffle
28
29 340 maturation, the subsequent winter harvest depends on the amount of the preceding summer
30
31 341 precipitation (Büntgen et al., 2019). Therefore, rapid summer warming, and a long-term
32
33 342 precipitation decline in southern Europe will reduce the local truffle winter harvest by 39% and
34
35 343 in turn increase prices by 66% (Fig. 4). Although there will be a 56 and 81% decline in truffle
36
37 344 production in the western United States and Chile, our MLR models project a price change of
38
39 345 only -7 and +8%, most likely due to slower warming. Disparity between production rates and
40
41 346 the price levels is related to the fact that estimates of both variables depend only on climate,
42
43 347 while lacking any economic behaviour. Moreover, estimates in our models cannot reflect daily
44
45 348 climate variability and short-term tolerance of truffles to heat stress (Garcia-Barreda et al.,
46
47 349 2019) via drought-resistant strains (Mello et al., 2006). Due to the opposing relationship
48
49 350 between October–November precipitation totals and Mediterranean truffle winter yields
50
51 351 (Büntgen et al., 2019), we suggest that the harvest in some TGRs, including those in the
52
53 352 Southern Hemisphere (Rojas et al., 2019), could be enhanced by a future decrease of
54
55
56
57
58
59
60

1
2
3 353 precipitation in late autumn/early winter. This would be ‘good news’ for truffle industries in
4
5 354 eastern Australia and New Zealand, where a weaker rate of evaporation from soil, coupled with
6
7 355 positive precipitation anomalies are likely to mitigate shrinking water resources. That,
8
9 356 combined with slower temperature increase in summer will maintain winter truffle production
10
11 357 at a level comparable to 1997–2020 (+9.5 and -0.2 %). With a price increase (decrease) of only
12
13 358 19% (75%), eastern Australia (New Zealand) is likely to provide more affordable truffles (Fig.
14
15
16
17 359 4).

18
19 360 All TGRs will require intensive irrigation to mitigate the negative effects of the predicted
20
21 361 trends and extremes of anthropogenic climate change. Although current irrigation rates are
22
23 362 estimated to buffer some future moisture losses in some TGRs (Cook et al., 2020), sustaining
24
25 363 such rates will likely not be possible under the gradual warming-induced decline in (sub)surface
26
27 364 and ground water reserves (Trnka et al., 2018). This, added to enhanced water conflict from
28
29 365 other socio-economic factors and the expansion of plantations associated with changes in
30
31 366 agricultural land-use for other crops will challenge the additional water supplies, particularly in
32
33 367 the fast-warming TGRs in Europe, the United States, Chile and western South Africa, where
34
35 368 summer precipitation is projected to decline until 2100 CE. However, a surplus of water from
36
37 369 irrigation, not based on adequate knowledge of the truffle’s lifecycle combined with ineffective
38
39 370 cultivation techniques, might reduce the harvest through enhanced microbial decay (Eslick,
40
41 371 2013). Furthermore, even without high-intensity irrigation, spatially variable extreme
42
43 372 precipitation events in a warmer climate (Fig. 3) could super-saturate plantation soils, causing
44
45 373 surface erosion, reduced soil oxygen content, and alternation of the physiochemical properties
46
47 374 of soil associated with a decrease in the diversity and abundance of truffles (Barnes et al., 2018;
48
49 375 Yan et al., 2019). Therefore, the extent, frequency and intensity of irrigation in truffle
50
51 376 plantations should not only compensate for future summer precipitation deficits (e.g., estimated
52
53 377 ~430 m³ per hectare in Europe under RCP_{8.5}), but also incorporate understanding of edaphic
54
55
56
57
58
59
60

1
2
3 378 factors and ecophysiological adaptations of associated host partners, such as drought-controlled
4
5 379 rhizogenesis and hydraulic redistribution (Büntgen et al., 2019). We emphasise the necessity of
6
7 380 increasing knowledge of fungus-host interaction under future ecological range shifts and
8
9 381 phenological widening (Kausserud et al., 2012), as well as for changes in resource availability.
10
11 382 Nutrients for mycelial development, which starts earlier under warmer conditions, are depleted
12
13 383 over a longer period, limiting subsequent fruiting body growth, and reducing fungal abundance
14
15 384 and diversity (Gange et al., 2013; Damialis et al., 2015). Moreover, truffle growers should
16
17 385 account for potential indirect effects associated with pathogens (*L. cinnamomea*) (Büntgen et
18
19 386 al., 2019), especially for the cultivation of truffles in the conditions of rapid warming. On the
20
21 387 other hand, adaptation of the truffle industry should take advantage of existing measures, such
22
23 388 as the use of drought-tolerant host species. The sector should further benefit from elevational
24
25 389 shifts in suitable climatic conditions that have already been observed in other fungal species
26
27 390 (Diez et al., 2020).

28
29
30
31
32
33 391 In addition to implications for agriculture and ecology, climate-induced changes of the
34
35 392 global truffle sector will have wide-ranging economic consequences (Fig. 5). While the truffle
36
37 393 sector is vulnerable to global challenges such as the financial crash in 2007/2008 or the current
38
39 394 COVID-19 pandemic that resulted in both lower demands due to closures of businesses, and
40
41 395 harvest declines associated with less workforce, region-specific future climate developments
42
43 396 are likely to lead to large-scale shifts in global truffle production and trade. In particular, the
44
45 397 stability of the truffle sector will worsen in fast-warming regions with an estimated precipitation
46
47 398 and thus production decline such as in southern Europe, where plantations expand each year by
48
49 399 ~2,220 hectares and harvesting employs over ~210,000 people together with an even higher
50
51 400 number of truffle-searching dogs (Reyna and Garcia-Barreda, 2014). Conversely, expanding
52
53 401 TGRs such as those in eastern Australia and New Zealand will profit from increased production,
54
55 402 while new suitable regions in Turkey and the greater Caucasus region may benefit from starting
56
57
58
59
60

1
2
3 403 cultivation interest, though further educational support is required to encourage development
4
5 404 in areas without a history of truffle culture.
6

7
8 405 With increased human involvement in cultivation and eco- or myco-tourism, the prestige
9
10 406 and exclusivity of the truffle sector is expected to rise, as are the prices for high-quality truffles,
11
12 407 regardless of the impacts of climate change. This trend, however, requires careful management,
13
14 408 as unlawful harvesting and trading, together with the introduction of competitive truffle species
15
16 409 and the reduction of genetic diversity, could become serious threats to sustainable truffle
17
18 410 production and product quality protection, and will need robust legal regulation in both
19
20 411 established and emerging TGRs worldwide. With regional support being pivotal in coping and
21
22 412 capitalising on the predicted changes yet to come, our findings offer a tool to inform future
23
24 413 policy, investment and decision-making in the development sustainable, optimised, global
25
26 414 cultivation truffle management.
27
28
29

30 415

31 416 **5 Conclusion**

32
33 417 By the end of the 21st century, all TGRs are expected to experience significant climate change.
34
35 418 State-of-the-art model simulations project 2.3 million km² of suitable land for truffle growth
36
37 419 will experience 50% faster aridification than the rest of the global land surface, with
38
39 420 significantly more heat waves between 2070 and 2099 CE. Global truffle production rates will
40
41 421 decrease by ~15%, while associated price levels will increase by ~36%. At the same time, a
42
43 422 predicted increase in summer precipitation and less intense warming over Australasia will likely
44
45 423 alleviate water scarcity and support higher yields of more affordable truffles. Our findings are
46
47 424 relevant for truffle farmers and businesses to adapt their irrigation systems and management
48
49 425 strategies to a warmer and drier future.
50
51
52
53
54
55

56 426

57 427 **Data availability statement**

1
2
3 428 All data used in this study are included in the article and its online supplementary materials.
4
5
6 429

7
8 430 **References**

- 9
10 431 Almazroui M, Saeed F, Saeed S, Islam MN, Ismail M, Klutse NAB and Siddiqui MH 2020
11
12 432 Projected Change in Temperature and Precipitation Over Africa from CMIP6. *Earth Syst.*
13
14 433 *Environ.* **4** 455–475
- 15
16
17 434 Andrys J, Kala J and Lyons TJ 2017 Regional climate projections of mean and extreme climate
18
19 435 for the southwest of Western Australia (1970–1999 compared to 2030–2059) *Clim. Dyn.* **48**
20
21 436 1723–1747
- 22
23
24 437 Araya-Osses D, Casanueva A, Román-Figueroa C, Uribe JM and Paneque M 2020 Climate
25
26 438 change projections of temperature and precipitation in Chile based on statistical
27
28 439 downscaling *Clim. Dyn.* **54** 4309–4330
- 29
30
31 440 Barnes CJ, van der Gast CJ, McNamara NP, Rowe R and Bending GD 2018 Extreme rainfall
32
33 441 affects assembly of the root-associated fungal community *New Phytol.* **220** 1172–1184
- 34
35
36 442 Beal LM, De Ruijter WPM, Biastoch A, Zahn R and SCOR/WCRP/IAPSO Working Group
37
38 443 136 2011 On the role of the Agulhas system in ocean circulation and climate *Nature* **472**
39
40 444 429–436
- 41
42
43 445 Beck H, Zimmermann NE, McVicar TR, Vergopolan N, Berg A and Wood EF 2018 Present
44
45 446 and future Köppen-Geiger climate classification maps at 1-km resolution. *Sci. Data* **5**
46
47 447 180214
- 48
49 448 Berg A, Sheffield J and Milly PCD 2016 Divergent surface and total soil moisture projections
50
51 449 under global warming *Geophys. Res. Lett.* **44** 236–244
- 52
53
54 450 Büntgen U and Egli S 2014 Breaking new ground at the interface of dendroecology and
55
56 451 mycology *Trends Plant Sci.* **19** 613–614
57
58
59
60

- 1
2
3 452 Büntgen U, Oliach D, Martínez-Peña F, Latorre J, Egli S and Krusic PJ 2019 Black truffle
4
5 453 winter production depends on Mediterranean summer precipitation *Environ. Res. Lett.* **14**
6
7 454 074004
8
9
10 455 Büntgen U, Egli S, Camarero JJ, Fischer EM, Stobbe U, Kauserud H, Tegel W, Sproll L and
11
12 456 Stenseth NC 2012 Drought-induced decline in Mediterranean truffle harvest *Nat. Clim.*
13
14 457 *Change* **2** 827–829
15
16
17 458 Büntgen U, Latorre J, Egli S and Martínez-Peña F 2017 Socio-economic, scientific, and
18
19 459 political benefits of mycotourism *Ecosphere* **8** e01870
20
21 460 Cai W *et al* 2020 Climate impacts of the El Niño–Southern Oscillation on South America *Nat.*
22
23 461 *Rev. Earth Environ.* **1** 215–231
24
25
26 462 Čejka T, Trnka M, Krusic PJ, Stobbe U, Oliach D, Václavík T and Tegel W 2020 Predicted
27
28 463 climate change will increase the truffle cultivation potential in central Europe *Sci. Rep.* **10**
29
30 464 21281
31
32
33 465 Challinor AJ, Watson J, Lobell DB, Howden SM, Smith DR and Chhetri N 2014 A meta-
34
35 466 analysis of crop yield under climate change and adaptation *Nat. Clim. Change* **4** 287–291
36
37
38 467 Cook BI and Wolkovich EM 2016 Climate change decouples drought from early winegrape
39
40 468 harvests in France *Nat. Clim. Change* **6** 715–719
41
42
43 469 Cook BI, McDermid SS, Puma MJ, Williams AP, Seager R, Kelley M, Nazarenko L, Aleinov
44
45 470 I 2020 Divergent Regional Climate Consequences of Maintaining Current Irrigation Rates
46
47 471 in the 21st Century *J. Geophys. Res. Atmos.* **125** e2019JD031814
48
49
50 472 Cook BI, Ault TR and Smerdon JE 2015 Unprecedented 21st century drought risk in the
51
52 473 American Southwest and Central Plains *Sci. Adv.* **1** e1400082
53
54
55 474 Cramer W *et al* 2018 Climate change and interconnected risks to sustainable development in
56
57 475 the Mediterranean *Nat. Clim. Change* **8** 972–980
58
59
60

- 1
2
3 476 Damialis A, Mohammad AB, Halley JM, and Gange AC 2015 Fungi in a changing world:
4
5 477 growth rates will be elevated, but spore production may decrease in future climates *Int. J.*
6
7 478 *Biometeorol.* **59** 1157–1167
- 9
10 479 Delworth TL and Zeng F 2014 Regional rainfall decline in Australia attributed to anthropogenic
11
12 480 greenhouse gases and ozone levels *Nat. Geosci.* **7** 583–587
- 14
15 481 Dey R, Lewis SC, Arblaster JM and Abram NJ 2019 A review of past and projected changes in
16
17 482 Australia’s rainfall *WIREs Clim. Change* **10** e577
- 18
19 483 Diez JM, James TY, McMunn M and Ibáñez I 2013 Predicting species-specific responses of
20
21 484 fungi to climatic variation using historical records *Glob. Change Biol.* **19** 3145–3153
- 23
24 485 Diez JM, Kauserud H, Andrew C, Heegaard E, Krisai-Greilhuber I, Senn-Irlet B, Høiland K,
25
26 486 Egli S and Büntgen U 2020 Altitudinal upwards shifts in fungal fruiting in the Alps *Proc.*
27
28 487 *Royal Soc. B.* **287** 20192348
- 30
31 488 Dosio A, Jones RG, Jack C, Lennard C, Nikulin G and Hewitson 2019 What can we know
32
33 489 about future precipitation in Africa? Robustness, significance and added value of
34
35 490 projections from a large ensemble of regional climate models *Clim. Dyn.* **53** 5833–5858
- 37
38 491 Eslick H 2013 *Identification and management of the agent causing rot in black truffles Part 2*
39
40 492 (Canberra: Union Offset Printing)
- 42
43 493 Fischer EM and Schär C 2010 Consistent geographical patterns of changes in high-impact
44
45 494 European heatwaves *Nat. Geosci.* **3** 398–403
- 46
47 495 Flato G and Marotzke J 2013 Evaluation of Climate Models. in *IPCC. Climate Change 2013:*
48
49 496 *The Physical Science Basis. Contribution of Working Group I to the Fifth Assessment*
50
51 497 *Report of the Intergovernmental Panel on Climate Change* (eds. Stocker TF, Qin D, Plattner
52
53 498 GK, Tignor M, Allen SK, Boschung J, Nauels A, Xia Y, Bex V and Midgley PM) 741–866
54
55 499 (Cambridge: Cambridge University Press)

- 1
2
3 500 Gange AC, Mohammad AB, Damialis A and Gange EG 2013 Mushroom phenological changes:
4
5 501 A role for resource availability? *PNAS* **110** E333–E334
6
7
8 502 Garcia-Barreda S and Camarero JJ 2020 Tree ring and water deficit indices as indicators of
9
10 503 drought impact on black truffle production in Spain *For. Ecol. Manag.* **475** 118438
11
12 504 Garcia-Barreda S, Sánchez S, Marco P and Serrano-Notivoli R 2019 Agro-climatic zoning of
13
14 505 Spanish forests naturally producing black truffle *Agric. For. Meteorol.* **269–270** 231–238
15
16
17 506 Gornall J, Betts R, Burke E, Clark R, Camp J, Willett K and Wiltshire A 2010 Implications of
18
19 507 climate change for agricultural productivity in the early twenty-first century *Philos. Trans.*
20
21 508 *R. Soc. Lond. B. Biol. Sci.* **365** 2973–2989
22
23
24 509 Hall IR, Yun W and Amicucci A 2003 Cultivation of edible ectomycorrhizal mushrooms
25
26 510 *Trends Biotechnol.* **21** 433–438
27
28 511 Hewitson BC and Crane RG 2006 CONSENSUS BETWEEN GCM CLIMATE CHANGE
29
30 512 PROJECTIONS WITH EMPIRICAL DOWNSCALING: PRECIPITATION
31
32 513 DOWNSCALING OVER SOUTH AFRICA *Int. J. Climatol.* **26** 1315–1337
33
34
35 514 Jacob D *et al* 2014 EURO-CORDEX: new high-resolution climate change projections for
36
37 515 European impact research *Reg. Environ. Change* **14** 563–578
38
39
40 516 Karavani A, De Cáceres M, de Aragón JM, Bonet JA and de-Miguel S 2018 Effect of climatic
41
42 517 and soil moisture conditions on mushroom productivity and related ecosystem services in
43
44 518 Mediterranean pine stands facing climate change *Agric. For. Meteorol.* **248** 432–440
45
46
47 519 Kauserud H *et al* 2012 Warming-induced shift in European mushroom fruiting phenology *Proc.*
48
49 520 *Natl. Acad. Sci.* **109** 14488–14493
50
51 521 King DA, Karoly DJ and Henley BJ 2017 Australian climate extremes at 1.5 °C and 2 °C of
52
53 522 global warming *Nat. Clim. Change* **7** 412–416
54
55
56 523 Le Tacon F, Marçais B, Courvoisier M, Murat C, Montpied P and Becker M 2014 Climatic
57
58 524 variations explain annual fluctuations in French Périgord black truffle wholesale markets
59
60

- 1
2
3 525 but do not explain the decrease in black truffle production over the last 48 years *Mycorrhiza*
4
5 526 **24** 115–125
6
7
8 527 Lefevre C 2012 Native and Cultivated Truffles of North America. in *Edible Ectomycorrhizal*
9
10 528 *Mushrooms. Current Knowledge and Future Perspectives* (eds. Zambonelli A and Bonito
11
12 529 GM) 209–227 (Berlin, Heidelberg: Springer)
13
14 530 Levene H 1960 Robust Tests for Equality of Variances. in *Contributions to Probability and*
15
16 531 *Statistics: Essays in Honor of Harold Hotelling* (ed. Olkin I) 278–292 (Redwood: Stanford
17
18 532 University Press)
19
20
21 533 Malajczuk N and Amaranthus M 2007 Cultivation of Tuber species in Australia. in *La culture*
22
23 534 *de La truffe dans Le monde* (ed. Chevalier G) 9–18 (Brive-La-Gaillarde: Ministère de la
24
25 535 Culture)
26
27
28 536 Mann HB 1945 Nonparametric tests against trend *Econometrica* **13** 245–259
29
30 537 Mann ME and Gleick PH 2015 Climate change and California drought in the 21st century *PNAS*
31
32 538 **112** 3858–3859
33
34
35 539 Mello A, Murat C and Bonfante P 2006 Truffles: much more than a prized and local fungal
36
37 540 delicacy *FEMS Microbiol. Lett.* **260** 1–8
38
39
40 541 Ministry for the Environment 2018 Climate Change Projections for New Zealand: Atmosphere
41
42 542 Projections Based on Simulations from the IPCC Fifth Assessment, 2nd Edition
43
44 543 (Wellington: Ministry for the Environment)
45
46
47 544 Morales-Castilla I, de Cortázar-Atauri IG, Cook BI, Lacombe T, Parker A, van Leeuwen C,
48
49 545 Nicholas KA and Wolkowich EM 2020 Diversity buffers winegrowing regions from
50
51 546 climate change losses *Proc. Natl. Acad. Sci.* **117** 2864–2869
52
53
54 547 Net W 2009 Rainfall trends in the KwaZulu-Natal Drakensberg region of South Africa during
55
56 548 the twentieth century *Int. J. Climatol.* **29** 1634–1641
57
58
59
60

- 1
2
3 549 Oliach D, Colinas C, Castaño C, Fischer CR, Bolaño F, Bonet JA and Oliva J 2020a The
4
5 550 influence of forest surroundings on the soil fungal community of black truffle (*Tuber*
6
7 551 *melanosporum*) plantations *For. Ecol. Manag.* **469** 188199
- 8
9
10 552 Oliach D *et al* 2020b Las trufas y las turmas. in *Los productos forestales no madereros en*
11
12 553 *España: Del monte a la industria* (eds. Sánchez-González M, Calama R. and Bonet JA)
13
14 554 283–324 (Madrid: Ministerio de Ciencia e Innovación)
- 15
16
17 555 Oliach D, Vidale E, Brenko A, Marois O, Andrighetto N, Stara K, de Aragón JM, Colinas C
18
19 556 and Bonet JA 2021 Truffle Market Evolution: An Application of the Delphi Method
20
21 557 *Forests* **12** 1174
- 22
23
24 558 Pascale S, Kapnick SB, Delworth TL and Cooke WF 2020 Increasing risk of another Cape
25
26 559 Town “Day Zero” drought in the 21st century *Proc. Natl. Acad. Sci.* **117** 29495–29503
- 27
28 560 Ponti L, Gutierrez AP, Ruti PM and Dell’Aquila A 2015 Fine-scale ecological and economic
29
30 561 assessment of climate change on olive in the Mediterranean Basin reveals winners and
31
32 562 losers *Proc. Natl. Acad. Sci.* **111** 5598–5603
- 33
34
35 563 QGIS.org 2021 QGIS Geographic Information System *QGIS Association* **3.16**
- 36
37 564 Raut BA, Reeder MJ and Jakob C 2017 Trends in CMIP5 Rainfall Patterns over Southwestern
38
39 565 Australia *J. Clim.* **30** 1779–1788
- 40
41
42 566 Ray DK, Gerber JS, MacDonald, GK and West PC 2015 Climate variation explains a third of
43
44 567 global crop yield variability *Nat. Commun.* **6** 5989
- 45
46
47 568 Reyna S 2012 Truficultura. Fundamentos y técnicas. 2a edición (Madrid: Mundi-Prensa)
- 48
49 569 Reyna S and Garcia-Barreda S 2014 Black truffle cultivation: a global reality *For. Syst.* **23** 317–
50
51 570 328
- 52
53
54 571 Roffe SJ, Fitchett JM and Curtis CJ 2019 Classifying and mapping rainfall seasonality in South
55
56 572 Africa: a review. *South African Geographical Journal* **101** 158–174
- 57
58
59
60

- 1
2
3 573 Rojas M, Lambert F, Ramirez-Villegas J and Challinor AJ 2019 Emergence of robust
4
5 574 precipitation changes across crop production areas in the 21st century *Proc. Natl. Acad.*
6
7 575 *Sci.* **116** 6673–6678
8
9
10 576 Salinger JM *et al* 2019 The unprecedented coupled ocean-atmosphere summer heatwave in the
11
12 577 New Zealand region 2017/18: drivers, mechanisms and impacts *Environ. Res. Lett.* **14**
13
14 578 044023
15
16
17 579 Sansom J and Renwick JA 2007 Climate Change Scenarios for New Zealand Rainfall *J. Appl.*
18
19 580 *Meteorol. Climatol.* **46** 573–590
20
21
22 581 Schulzweida U 2019 CDO User Guide *Max Planck Institute* **1.9.8.**
23
24 582 Shapiro SS and Wilk MB 1965 An analysis of variance test for normality (complete samples)
25
26 583 *Biometrika* **52** 591–611
27
28
29 584 Thomas P and Büntgen U 2019 A risk assessment of Europe's black truffle sector under
30
31 585 predicted climate change *Sci. Total Environ.* **655** 27–34
32
33
34 586 Thomas P and Büntgen U 2017 First harvest of Périgord black truffle in the UK as a result of
35
36 587 climate change *Clim. Res.* **74** 67–70
37
38
39 588 Timbal B, Fiddes S and Brown JR 2017 Understanding south-east Australian rainfall projection
40
41 589 uncertainties: the influence of patterns of projected tropical warming *Int. J. Climatol.* **37**
42
43 590 921–939
44
45
46 591 Trnka M *et al* 2018 Priority questions in multidisciplinary drought research *Clim. Res.* **75** 241–
47
48 592 260
49
50
51 593 Tuel A and Eltahir EAB 2020 Why Is the Mediterranean a Climate Change Hot Spot? *J. Clim.*
52
53 594 **33** 5829–5843
54
55
56 595 Wang F, Shao W, Yu H, Kan G, He X, Zhang D, Ren M and Wang G 2020 Re-evaluation of
57
58 596 the Power of the Mann-Kendall Test for Detecting Monotonic Trends in
59
60 597 Hydrometeorological Time Series *Front. Earth Sci.* **8** 1–12

1
2
3 598 Yan T, Qu T, Song H, Sun Z, Zeng H and Peng S 2019 Ectomycorrhizal fungi respiration
4
5 599 quantification and drivers in three differently-aged larch plantations *Agric. For. Meteorol.*
6
7 600 **265** 245–251

8
9
10 601 Zhang H and Delworth TL 2018 Robustness of anthropogenically forced decadal precipitation
11
12 602 changes projected for the 21st century *Nat. Commun.* **9** 1–10

13
14 603

15 16 17 604 **Acknowledgements**

18
19 605 This study was supported by the projects “SustES – Adaptation strategies for sustainable
20
21 606 ecosystem services and food security under adverse environmental conditions”
22
23 607 (CZ.02.1.01/0.0/0.0/16_019/0000797) and “Geografický výzkum dynamiky přírodních a
24
25 608 společenských prostorových procesů (GEODYN)” (MUNI/A/1570/2020). UB received
26
27 609 additional funding from the ERC Advanced project Monostar (AdG 882727).

28
29
30 610

31 32 33 611 **Author contributions**

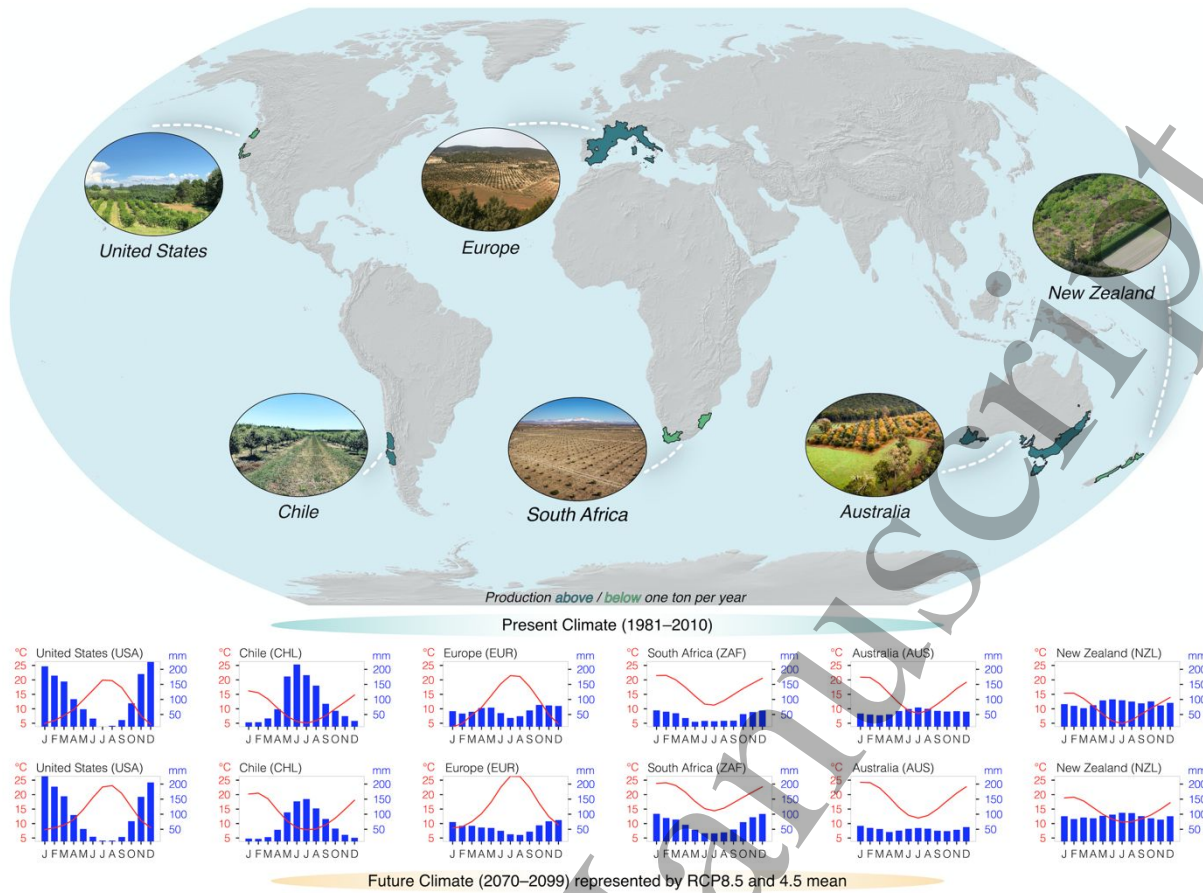
34
35 612 UB conceived the main idea and TČ designed and carried out the analyses. TČ wrote the
36
37 613 manuscript with input from EI, DO, SE, FMP, MT, PT and UB. All authors contributed
38
39 614 critically to the discussion and interpretation of the results, and approved submission.

40
41
42 615

43 44 45 616 **Competing interests**

46
47 617 The authors declare no competing interests.

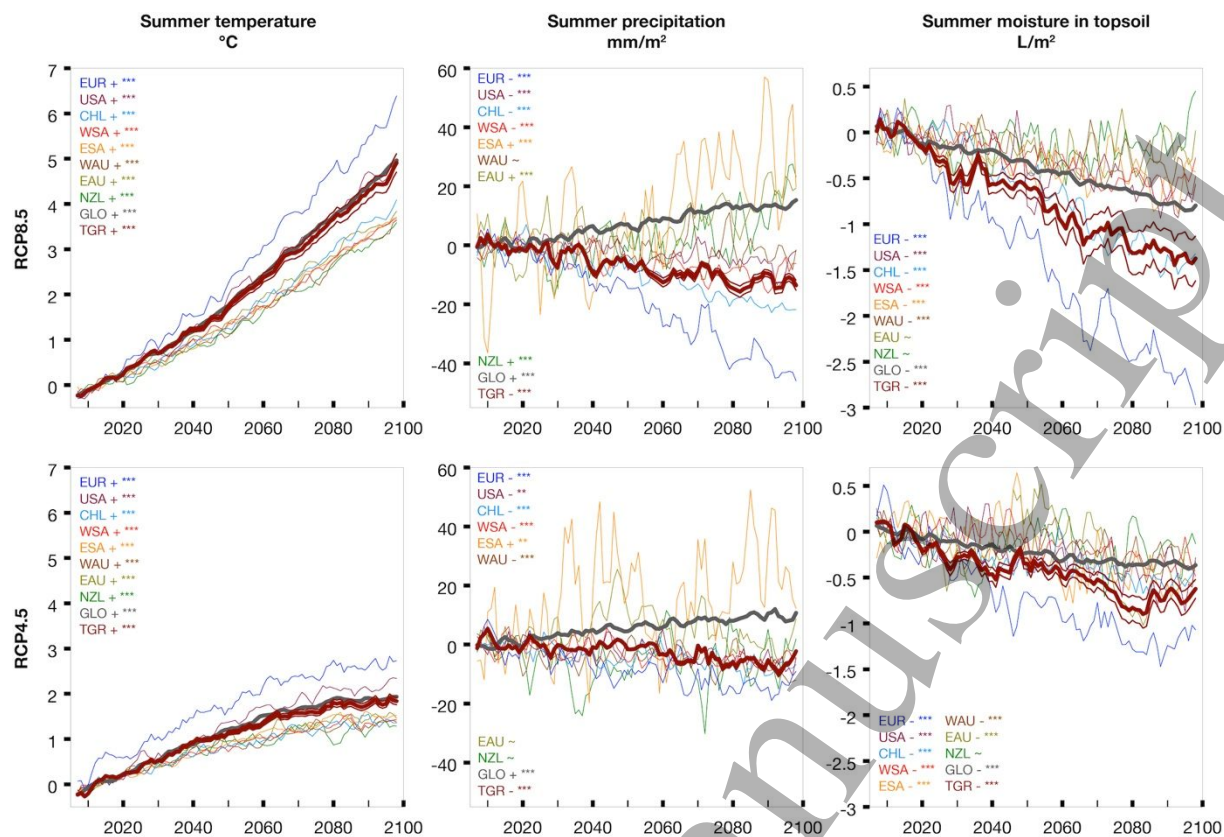
48
49 618
50
51
52
53
54
55
56
57
58
59
60



619

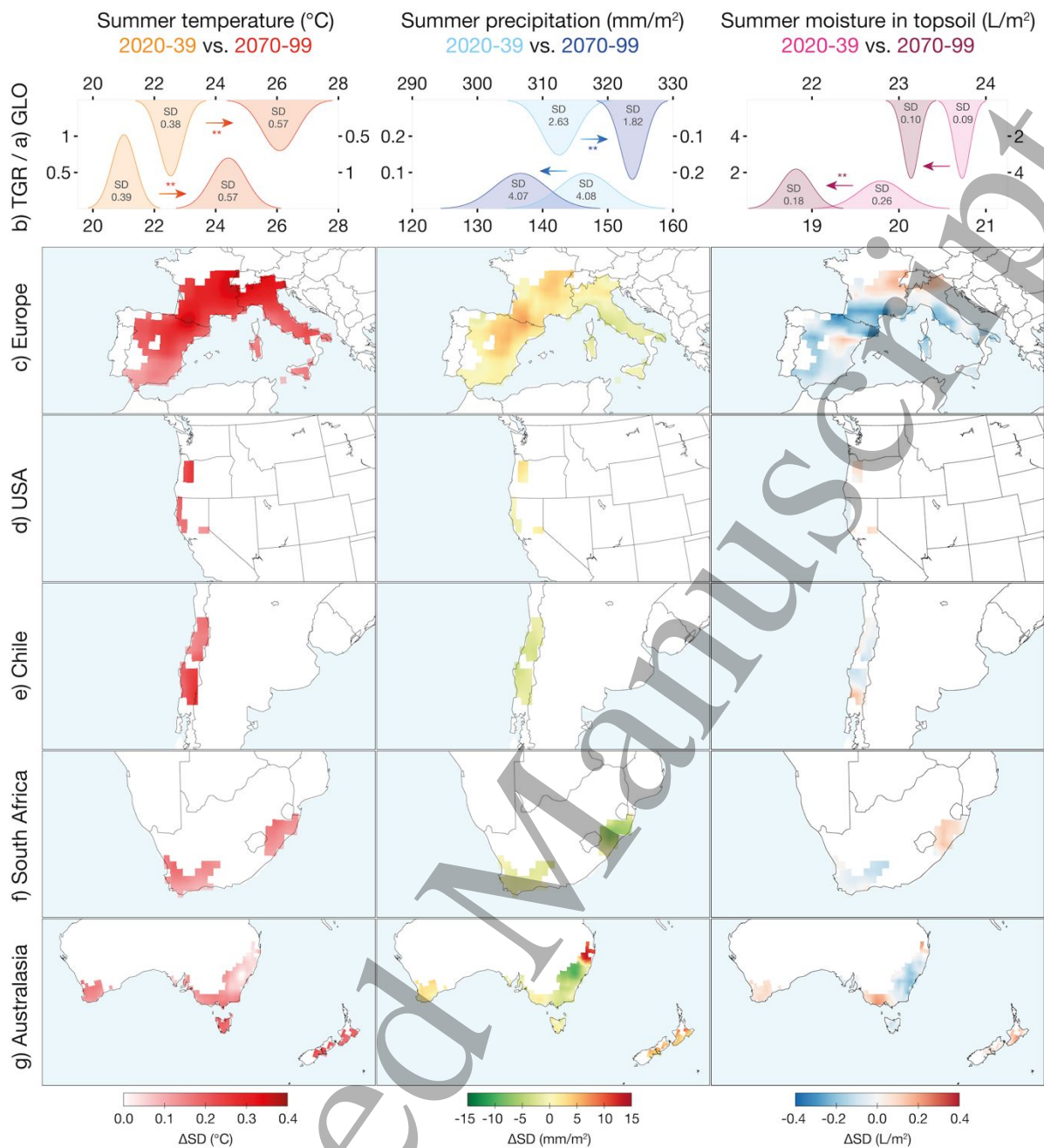
620 **Figure 1 | Truffle regions.** Coupled with the corresponding climate diagrams characterising a
 621 monthly temperature means and precipitation totals for ‘present’ (1981–2010; upper row) and
 622 ‘future’ climate (2070–2099; lower row). Photo courtesy of G. Booth (Australia), W. Tewnton
 623 (New Zealand), S. O’Toole (California), R. Ramírez (Chile), P. Miros (South Africa), and D.
 624 Oliach (Europe).

625



626
 627 **Figure 2 | Climate projections.** Bias-corrected predicted summer temperature ($^{\circ}\text{C}$),
 628 precipitation (mm) and moisture in upper portion (~ 10 cm) of soil column ($\text{L} \cdot \text{m}^{-2}$) under RCP_{4.5}
 629 and RCP_{8.5}. The 2006–2099 data (X-axis: smoothed by 3-yr running average) are presented as
 630 anomalies relative to the 2006–2020 baseline mean. While coloured thin lines symbolise the
 631 individual truffle regions, the bold-transparent red and grey contours represent the truffle (TGR
 632 = all truffle growing regions combined) and the remaining global land surface (GLO),
 633 respectively. The GLO for soil moisture excludes Antarctica and TGR is accompanied by
 634 confidence intervals (95%) to show the variability between GCMs. Statistically significant
 635 increasing (+) or decreasing (-) trend is symbolised with an asterisk (** = 95%, *** = 99%) of
 636 a non-seasonal Mann-Kendall trend test (applied for 2006–2099).

637



638

639 **Figure 3 | Climate variability.** Expected change in interannual variability (RCP_{8.5}) of summer

640 temperature, precipitation, and moisture in the upper ~10 cm of the soil column, expressed as

641 the difference in standard deviation between the early (2010–2039) and late (2070–2099)

642 periods. **a–b:** Distribution functions (adjusted for bias) are calculated from the mean and

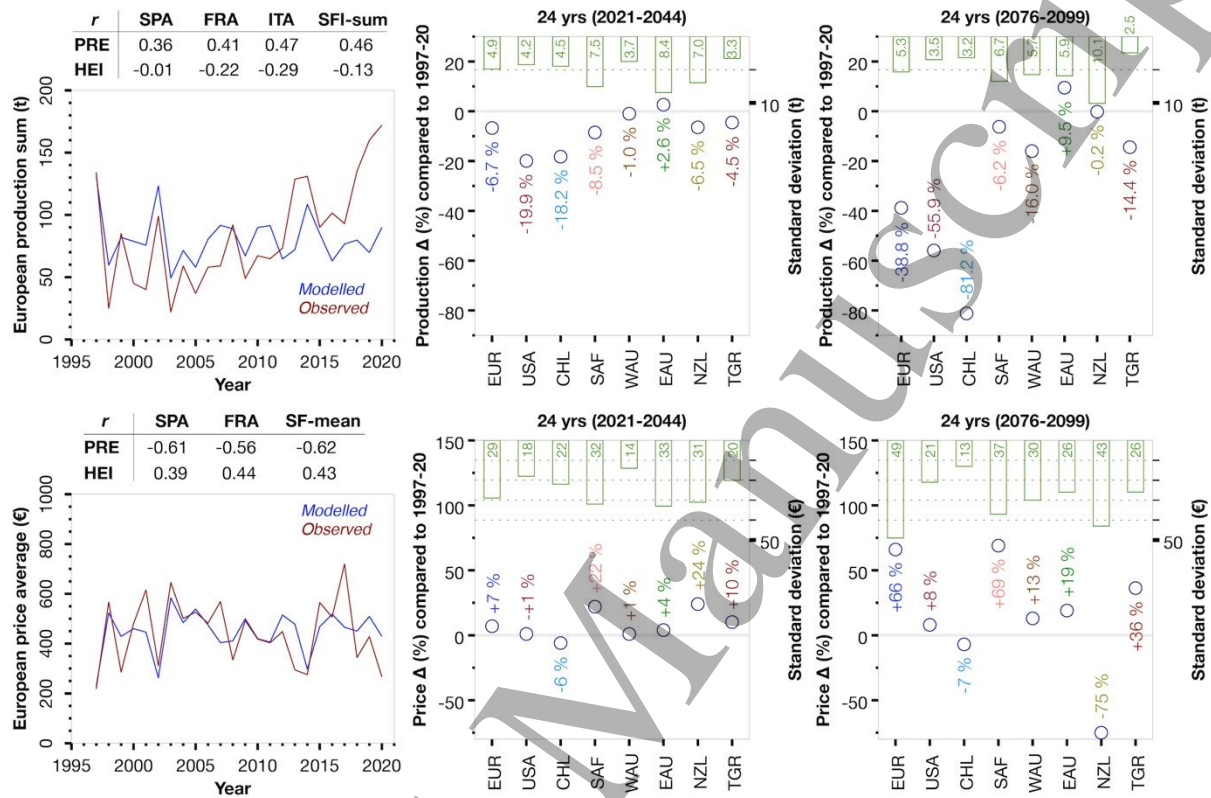
643 standard deviation for each period after calculating the area-average of all truffle-growing

644 regions (TGR) and the remaining global land surface (GLO). Statistically significant difference

645 in variance (non-parametric Levene's test) is symbolised with an asterisk (** = 95%). **c–g:**

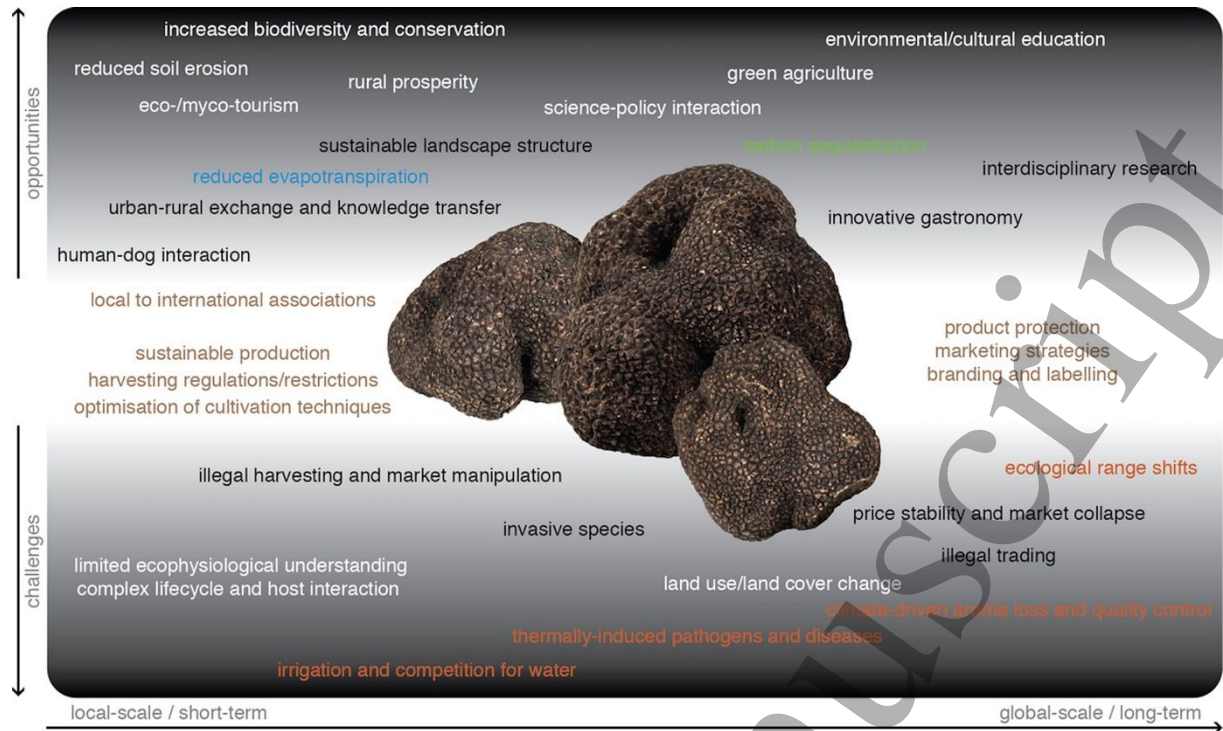
646 Spatial distribution of climate extremes expressed as the positive (increasing) or negative
 647 (decreasing) difference in standard deviation between two periods for all grid cells in each
 648 truffle-growing region.

649



650
 651 **Figure 4 | Truffle market.** (Left) Agreement between observed and modelled truffle
 652 production rates in Europe (sum of Spanish, French and Italian data) and price levels (average
 653 of Spanish and French records) for the period 1997–2020 (24 years). The individual correlations
 654 between national datasets (SPA, FRA, ITA), European aggregates (SFI-sum and SF-mean),
 655 summer precipitation totals (PRE) and heat index (HI) are shown above the graphs. (Middle)
 656 The blue circles are the estimated differences (in %) in production rates (top) and price levels
 657 (bottom) for the near future (2021–2044) compared to the period 1997–2020. The green bars
 658 represent the standard deviation calculated over 24 years for this period. (Right) Similar to
 659 (Middle) but targeting the end of the 21st century (2076–2099).

660



661
 662 **Figure 5 | Risk and reward of the emerging truffle sector.** Global (long-term) and local
 663 (short-term) challenges and opportunities under social, management, and scientific perspective
 664 of truffle hunting and cultivation.